AIP | Applied Physics Letters

Near-field characterization of chemical vapor deposition graphene in the microwave regime

Anestis Katsounaros, Matthew T. Cole, Hatice M. Tuncer, William I. Milne, and Yang Hao

Citation: Appl. Phys. Lett. **102**, 233104 (2013); doi: 10.1063/1.4810759
View online: http://dx.doi.org/10.1063/1.4810759
View Table of Contents: http://apl.aip.org/resource/1/APPLAB/v102/i23
Published by the American Institute of Physics.

Near-field characterization of chemical vapor deposition graphene in the microwave regime

Anestis Katsounaros,[1] Matthew T. Cole,[2] Hatice M. Tuncer,[2] William I. Milne,[2] and Yang Hao[1,a)]
[1]*School of Electronic Engineering and Computer Science, Queen Mary, University of London, Mile End Road, London E1 4NS, United Kingdom*
[2]*Department of Engineering, University of Cambridge, 9 JJ Thomson Avenue, Cambridge CB3 0FA, United Kingdom*

(Received 29 November 2012; accepted 26 May 2013; published online 12 June 2013)

Near-field measurements were performed at X-band frequencies for graphene on copper microstrip transmission lines. An improvement in radiation of 0.88 dB at 10.2 GHz is exhibited from the monolayer graphene antenna which has dc sheet resistivity of 985 Ω/sq. Emission characteristics were validated via *ab initio* simulations and compared to empirical findings of geometrically comparable copper patches. This study contributes to the current knowledge of the electronic properties of graphene. © *2013 AIP Publishing LLC*. [http://dx.doi.org/10.1063/1.4810759]

Graphene is a two–dimensional, single atomic thick layer of hexagonally latticed carbon atoms. Since its unexpected existence was verified, focus has shifted toward retrofitting graphene—with all its unique electrical, optical and mechanical properties[1–5]—into existing technologies such as liquid crystal devices,[6] transistors and analogue logic,[7] supercapacitors,[8] and electronic mixers.[9]

The development of integrated radio devices necessitates the production of highly crystalline graphene over large areas. Graphene can be isolated by successive removal of graphite layers or by the self-assembly of single molecular units. To date, various derivatives of these have been demonstrated, including; micromechanical and liquid phase exfoliation,[10] epitaxial growth,[11] as well as plasma[12] and flame assisted[13] techniques. However, chemical vapour deposition (CVD)[14] shows perhaps the most promise in terms of scalability. Mechanical exfoliation provides high quality crystalline graphene, which are unsuitably small (tens of μm). Epitaxy requires expensive substrates, ultrahigh vacuum, and high temperature[15] processing. Growth by CVD provides the most popular, cost effective, and technologically feasible method available. The interesting properties of graphene have been explored for a range of applications in the high–GHz and optical frequencies.[6,16–19] Here, we investigate the possibility of using graphene as a radiating element at X–band frequencies.

Graphene was synthesised by thermal CVD in a cold–walled, commercially available reactor (Aixtron Ltd., Black Magic). 500 nm–thick copper was magnetron sputtered onto 200 nm thermally oxidised Si ⟨100⟩ subsequently annealed at 850 °C for 30 min in a 20:1500 standard cubic centimeters per minute H_2:Ar atmosphere at 4 mbar.[20] Graphene growth was initiated by introducing 7 sccm CH_4 (99.9%) under maintained H_2 (99.98%) and Ar (99.998%) dilution. All samples were cooled to room temperature under ultra–high purity N_2 (99.999%). Temperatures were monitored using two type K bimetallic thermocouples and a surface infrared interferometer. Pressures and temperatures were accurate to within ±0.1 mbar and ±1 °C, respectively. Standard FeCl wet–etching and poly (methyl methacrylate)–mediated graphene transfer were used.[21] Raman spectroscopy (Renishaw InVia) was performed on the as-grown and transferred graphene at 457 nm (2.71 eV), 532 nm (2.33 eV), and 633 nm (1.96 eV), with an incident power <3 mW. 50 Ω microstrip transmission lines were printed on 1.58 mm thick Duroid ($\epsilon = 2.2$, $\tan\delta = 9 \times 10^4$) and a rectangular graphene patch was placed on top (Fig. 1). Negligible defects were induced by the transfer process. Figure 2 shows a typical Raman spectra of the transferred graphene. Means $(\pm 1 s.d.)$ for the I_D/I_G, I_{2D}/I_G, and full-width half-maximum (FWHM) of the 2*D* peak ($\sim$2700 cm^{-1}) were extracted at each energy. Second order polynomial–like curves, associated with substrate electroluminescence were manually removed for clarity.

The graphene was 57.6% (by area) monolayer, 23.7% bilayer, and 18.7% few layer with mean $I_D/I_G = 0.11(\pm 0.02)$, $I_{2D}/I_G = 0.82(\pm 0.12)$, and a 2D FWHM of 49.2(±2.4) cm^{-1}, which suggests a high quality crystalline material. All 2D peaks, at all excitation energies, were well–fitted with single Lorentzians further supporting the presence of monolayer graphene. The dispersion relations (Fig. 2) indicate a highly crystalline material comparable to most exfoliated films.[22]

Detailed transmission line dimensions are shown in Fig. 1. An identical bare (without graphene) transmission line, as well

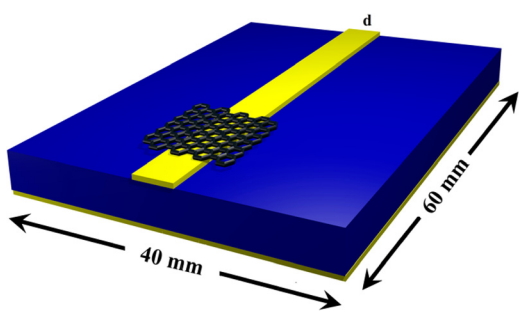

FIG. 1. Implemented microstrip transmission line on a 1.58 mm thick Duroid 5880. The 50 Ω transmission line is $d = 4.89$ mm wide and the graphene area is 9 mm × 10 mm.

a)yang.hao@eecs.qmul.ac.uk

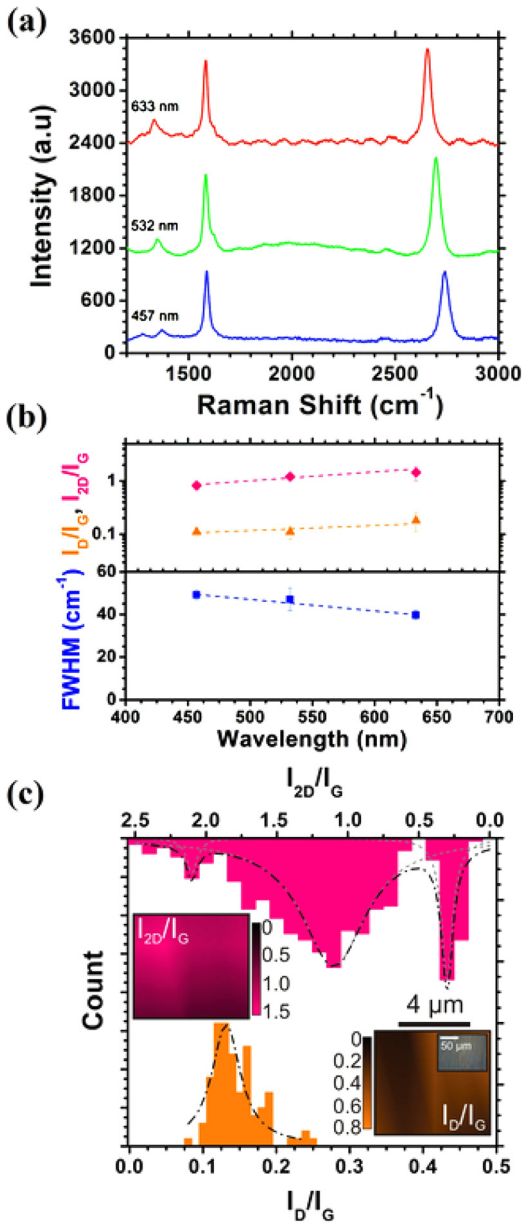

FIG. 2. (a) Raman spectra (<3 mW incident power) at 457 nm (2.71 eV), 532 nm (2.33 eV), and 633 nm (1.96 eV). (b) Dispersion relations of I_D/I_G, I_{2D}/I_G, and the 2D-FWHM. (c) Histogram (Count > 100 scans) of the I_D/I_G, single Lorentzian peak at 0.11(±0.02), and I_{2D}/I_G, showing a binary peak indicating the presence of monolayer and bilayer regions. Inset: Typical spatially resolved Raman maps (532 nm) of optical micrograph of transferred graphene on a Duroid substrate.

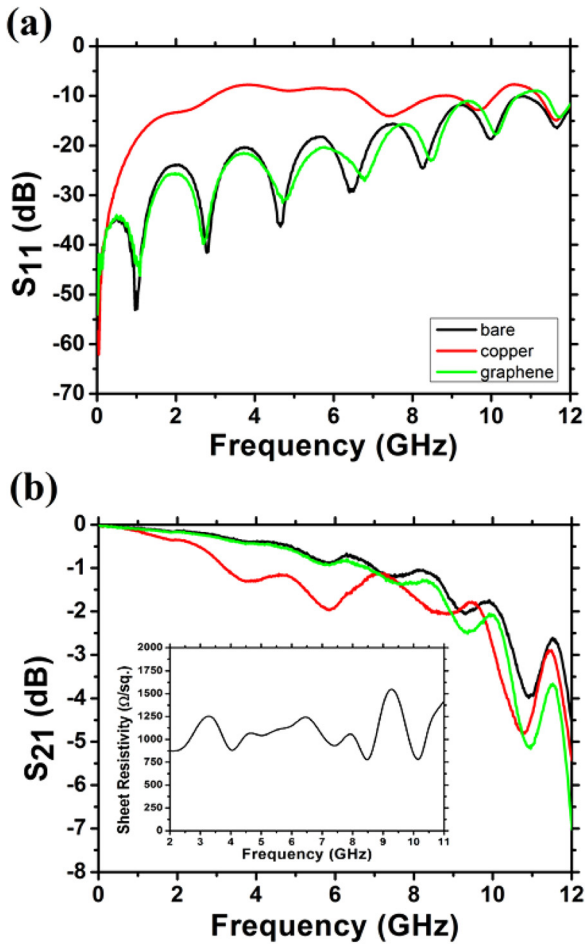

FIG. 3. (a) Reflection (*S*11) and (b) transmission (*S*21) coefficients of the bare transmission line (black), the graphene patch (green), and the copper patch (red). Inset: Optimized surface conductivity of graphene.

as an equivalent with a copper patch, located at the exact location of the graphene, were fabricated for comparison.

The S–parameters of the above devices were measured, as depicted in Fig. 3. The graphene enhances the dielectric losses. The impedance mismatch caused by the copper patch, as illustrated in Fig. 3(b), is similarly severe and increases reflections by at least 10 dB whilst reducing transmission by 1 dB.

The sheet resistivity of graphene is typically 1 kΩ/sq. in DC (Ref. 10) and around 700 Ω/sq. at optical frequencies.[23] An *ab initio* model (CST-Microwave Studio) was developed based on the structure illustrated in Fig. 1. Our empirical S–parameters (Fig. 3) were used as target conditions for optimization. A dimensionless cost function (fc) was specified relating sheet resistivity (Ω/sq.) to the S–parameters. fc was terminated for values $<10^{-6}$. The frequency step was set to 0.5 GHz. The optimized sheet resistivity is presented in the inset of Fig. 3(b). For an approximate linear fit, the dc sheet resistivity was 985 Ω/sq., which agrees with results in Ref. 10. Moreover, in microwave frequencies, the calculated surface resistance is also consistent with Refs. 24 and 25.

To study the radiation characteristics, a NSI–200 *V*–3 × 3 vertical planar scanner was used in the near field. The scanned area was set to 80 mm × 50 mm. Measurements were performed in the X–band (8–12 GHz) using an open ended NSI–RF–WR90 waveguide at a distance of 6 mm from the source plane and a spatial resolution of 1 mm. Near–field distributions (10.2 GHz) are shown in Fig. 4 for the bare (a), graphene (b), and Cu patch (c) structures described above.

Microstrip transmission lines are non-radiating structures. Thus, far–field measurements in an anechoic chamber are unlikely to be successful due to the large transmitter–receiver distance. Consequently, the most appropriate way to measure the radiation characteristics of such structures is to perform near-field measurements. Vertical and horizontal cross-sections of the three near–field patterns depicted in Fig. 4 are plotted, at 10.2 GHz, in Fig. 5. Similar behaviour was observed throughout the entire X–band.

Figure 6 clearly shows that the bare transmission line, and that of the graphene additive have very similar radiating characteristics at 8 GHz and 12 GHz. This consistent

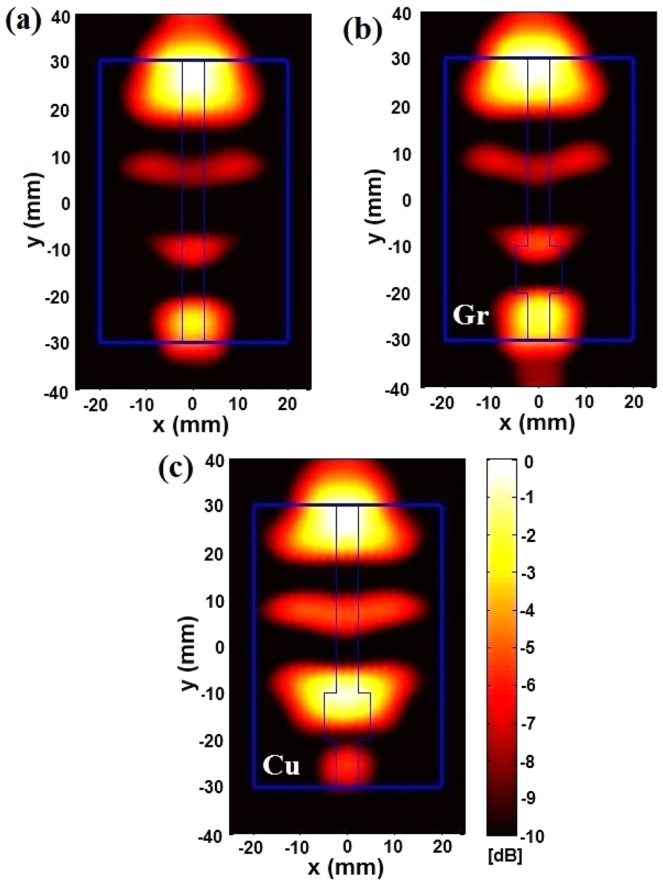

FIG. 4. Near-field plots (10.2 GHz) of; (a) bare microstrip transmission line, (b) the microstrip transmission line with a graphene (Gr) patch, and (c) the copper (Cu) patch. The blue overlay diagram has been added in each to denote the board and patch location.

behaviour deviates at around 10 GHz, where very weak radiation from the graphene is observed in the horizontal cross-section ($y = -10$ mm). The measurement has been repeated several times and an average maximum difference of 0.88 dB, occurring at 10.2 GHz, is observed. A horizontal cross–section of the same structure, at $y = 15$ mm is plotted in Fig. 5 for comparison, showing that the effect is indeed a product of the graphene. Evidently, graphene has relatively low conductivity at microwave frequencies compared to bulk copper.

This increase in radiation performance is attributed to the presence of the graphene which functions in a similar fashion to a radiating rectangular patch antenna. Here, the fundamental mode resonance frequency is described by[26]

$$f = \frac{c}{2 \cdot (L + h)\sqrt{\epsilon_{eff}}}, \tag{1}$$

where c is the speed of light, L is the patch resonant length, h is the height of the substrate, and ϵ_{eff} is the effective permittivity of the substrate with dielectric constant of ϵ_r given by

$$\epsilon_{eff} = \frac{\epsilon_r + 1}{2} + \frac{\epsilon r - 1}{2} \cdot \frac{1}{\sqrt{1 + 12 \cdot h/W}}. \tag{2}$$

The graphene patch is 9 cm × 10 cm. Thus, $\epsilon_{eff} = 1.87$ and $f = 10.36$ GHz which lies within an acceptable error where the maximum radiation occurred (Fig. 6). Considering

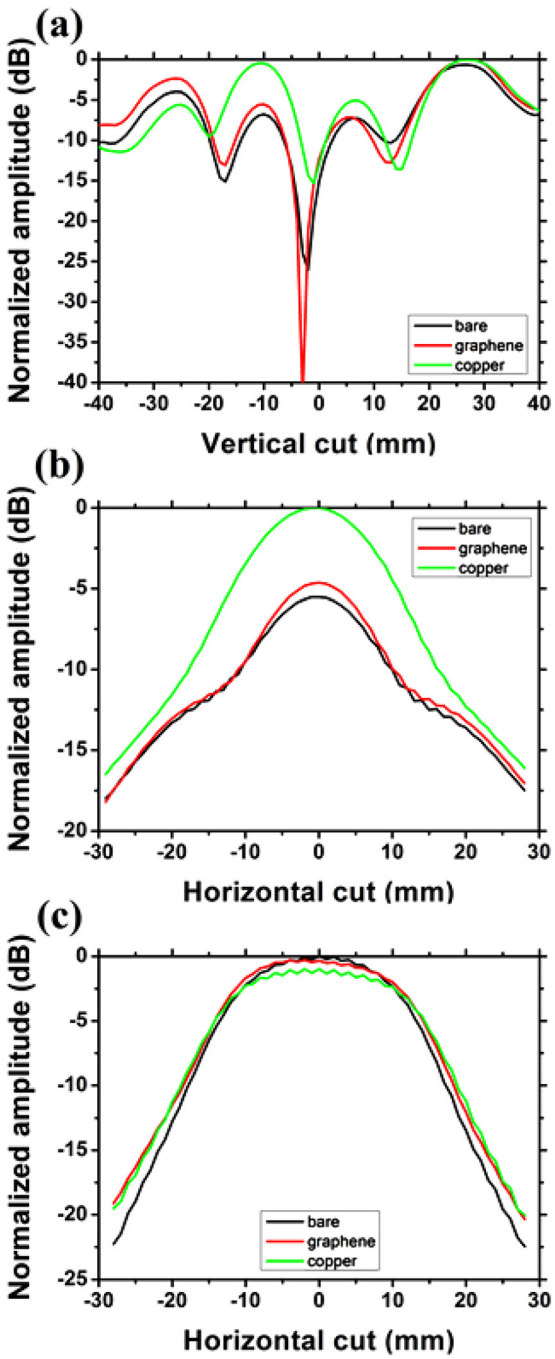

FIG. 5. Normalized amplitude at 10.2 GHz of (a) a vertical cross–section of the near field distribution taken at $x = 0$ mm. (b) A horizontal cross–section taken at $y = -10$ mm, through the graphene and copper patches. (c) A horizontal cross–section taken at $y = +15$ mm, far removed from the graphene and copper patches.

that the efficiency of a copper patch antenna will be around 80%, the radiation efficiency of an identical microstrip patch antenna made of graphene is estimated to be 20.7% at 10.2 GHz as shown in Fig. 6. This is in accordance with theoretical values given by Ref. 27. As expected, most of the input power is dissipated, therefore, graphene in X–band frequencies is dominated by losses.

Here, we have demonstrated near field X–band microwave emission measurements for rectangular graphene structures on copper microstrip transmission lines. The fundamental mode of the microstrip rectangular patch was found to

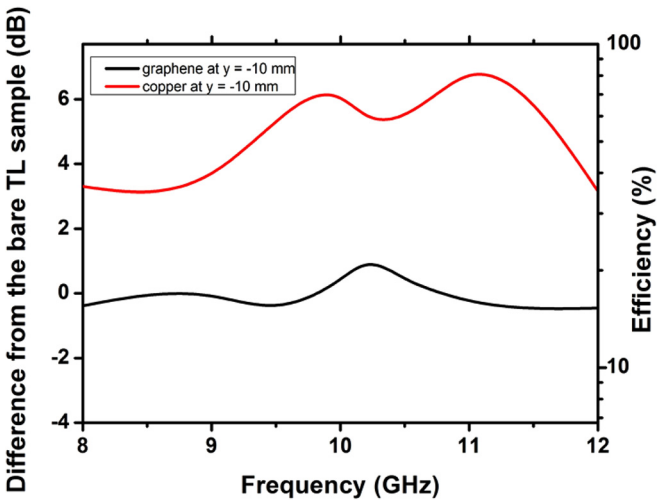

FIG. 6. Gain from graphene (black) and copper patch (red) at $y = -10$ mm. Estimated efficiency of a potential microstrip patch antenna made of graphene (black) and copper (red) is also presented.

be in the range where the maximum radiation of graphene occurs. The experimental verification of surface conductivity of graphene can lead to a variety of new microwave applications based on emergent graphene technologies.

M. T. Cole thanks the Isaac Newton Trust for generous financial support.

[1]A. K. Geim and K. S. Novoselov, Nature Mater. **6**, 183 (2007).
[2]K. S. Novoselov, A. K. Geim, S. V. Morozov, D. Jiang, M. I. Katsnelson, I. V. Grigorieva, S. V. Dubonos, and A. A. Firsov, Nature **438**, 197 (2005).
[3]Y. B. Zhang, Y. W. Tan, H. L. Stormer, and P. Kim, Nature **438**, 201 (2005).
[4]M. Dragoman and D. Dragoman, Prog. Quantum Electron. **33**, 165 (2009).
[5]P. Blake, E. W. Hill, A. H. C. Neto, K. S. Novoselov, D. Jiang, R. Yang, T. J. Booth, and A. K. Geim, Appl. Phys. Lett. **91**, 063124 (2007).
[6]P. Blake, P. D. Brimicombe, R. R. Nair, T. J. Booth, D. Jiang, F. Schedin, L. A. Ponomarenko, S. V. Morozov, H. F. Gleeson, E. W. Hill *et al.*, Nano Lett. **8**, 1704 (2008).
[7]Y. M. Lin, A. Valdes-Garcia, S. J. Han, D. B. Farmer, I. Meric, Y. N. Sun, Y. Q. Wu, C. Dimitrakopoulos, A. Grill, P. Avouris *et al.*, Science **332**, 1294 (2011).
[8]Y. W. Zhu, S. Murali, M. D. Stoller, A. Velamakanni, R. D. Piner, and R. S. Ruoff, Carbon **48**, 2118 (2010).
[9]H. Wang, A. Hsu, J. Wu, J. Kong, and T. Palacios, IEEE Electron Device Lett. **31**, 906 (2010).
[10]K. S. Novoselov, A. K. Geim, S. V. Morozov, D. Jiang, Y. Zhang, S. V. Dubonos, I. V. Grigorieva, and A. A. Firsov, Science **306**, 666–669 (2004).
[11]C. Berger, Z. M. Song, X. B. Li, X. S. Wu, N. Brown, C. Naud, D. Mayou, T. B. Li, J. Hass, A. N. Marchenkov *et al.*, Science **312**, 1191–1196 (2006).
[12]G. X. Zhao, D. D. Shao, C. L. Chen, and X. K. Wang, Appl. Phys. Lett. **98**, 183114 (2011).
[13]R. N. Tiwari, M. Ishihara, J. N. Tiwari, and M. Yoshimura, J. Mater. Chem. **22**, 15031 (2012).
[14]A. Ismach, C. Druzgalski, S. Penwell, A. Schwartzberg, M. Zheng, A. Javey, J. Bokor, and Y. G. Zhang, Nano Lett. **10**, 1542 (2010).
[15]P. Sutter, Nature Mater. **8**, 171 (2009).
[16]F. N. Xia, T. Mueller, Y. M. Lin, A. Valdes-Garcia, and P. Avouris, Nature Nanotechnol. **4**, 839 (2009).
[17]N. Papasimakis, Z. Q. Luo, Z. X. Shen, F. D. Angelis, E. D. Fabrizio, A. E. Nikolaenko, and N. I. Zheludev, Opt. Express **18**, 8353 (2010).
[18]D. R. Andersen, J. Opt. Soc. Am. B **27**, 818 (2010).
[19]G. W. Hanson, J. Appl. Phys. **104**, 084314 (2008).
[20]M. T. Cole, Ph.D. dissertation, Cambridge University, 2011.
[21]K. S. Kim, Y. Zhao, H. Jang, S. Y. Lee, J. M. Kim, K. S. Kim, J. H. Ahn, P. Kim, J. Y. Choi, and B. H. Hong, Nature **457**, 706 (2009).
[22]A. C. Ferrari, Solid State Commun. **143**, 47 (2007).
[23]A. Reina, X. T. Jia, J. Ho, D. Nezich, H. B. Son, V. Bulovic, M. S. Dresselhaus, and J. Kong, Nano Lett. **9**, 30 (2009).
[24]L. Hao, J. Gallop, S. Goniszewski, A. Gregory, O. Shaforost, N. Klein, and R. Yakimova, http://arxiv.org/abs/1304.1304, 2013.
[25]Z. Wu, L. Wang, I. Zimmerman, and H. Xin, in *Proceedings of SiRF 2011* (2011), pp. 181–184.
[26]C. A. Balanis, *Antenna Theory: Analysis and Design*, 3rd ed. (Wiley-Interscience, 2005).
[27]J. S. Gomez-Diaz and J. Perruisseau-Carrier, in *Proceedings of ISAP 2012, Nagoya, Japan* (2012), pp. 239–242.